Structural Health Monitoring of Aerospace Structural Components Using Wave Propagation Based Diagnostics

S. GOPALAKRISHNAN

ABSTRACT

The paper discusses a wave propagation based method for identifying the damages in an aircraft built up structural component such as delamination and skin-stiffener debonding. First, a spectral finite element model (SFEM) is developed for modeling wave propagation in general built-up structures by using the concept of assembling 2D spectral plate elements. The developed numerical model is validated using conventional 2-D FEM. Studies are performed to capture the mode coupling, that is, the flexural-axial coupling present in the wave responses. Lastly, the damages in these built up structures are then identified using the developed SFEM model and the measured responses using the concept Damage Force Indicator (DFI) technique.

INTRODUCTION

Present day aerospace vehicles are increasingly made of composites due to their high strength to weight and stiffness to weight ratios. In addition to reduced structural weight, they possess improved corrosion resistance. The assembly of composite structures is not a straight forward task. Unlike metallic structures, it is not easy and feasible to join different composite components using riveted joints and different cross-sectional angle plates. The incorporation of co-cured, co-bonded complex composite components in aviation vehicles have resulted in the total reduction of structural components by 40% compared to metallic structure. The type of composite stiffeners having cross sections such as T-joint, L-joints and hat sections are common in modern composite co-cured airframe structures. The purpose of these stiffened structures is to prevent skin buckling during wing loading and to increases the bending strength of the joint.

Gopalakrishnan Srinivasan, Indian Institute of Science, Bangalore 560 012, India

From the above discussion, we can see that the stiffened constructions are the building block of the wing sections of an aircraft. The structural health monitoring of these composite structures is a major challenge, faced by the aircraft industry. In case of composite structures, guided waves offer a great potential for health monitoring applications since they can propagate long distances with little attenuation and in addition, they can interact strongly even with small damage. Further, these waves can be excited and sensed by contact measurements such as piezoelectric elements that can be permanently attached onto a structure or through non-contact sensors such as SLDV and thus offering online monitoring capability. The structural health monitoring of stiffened plate structure and wing box structure, using guided wave technique can be found respectively in [1-2]. In these references, purely experimental results are reported and to the author's best knowledge, no numerical/analytical/semi-analytical model is reported in the literature, which is one of the objectives of the paper.

There are several numerical methods found in the archival of literature for the vibration analysis of stiffened plate and among them the Finite element (FE) based method has been found to be accurate with less complexity to model stiffened plates [3-5]. Not much work on wave propagation in stiffened structures is reported in the literature. The fundamental aspect of wave propagation in stiffened structures is that the wave scattering and mode coupling occurs at the web flange interfaces due to the different impedances of the flange and the web. In addition, if a debond occurs, in addition to the mode coupling due stiffener-skin connections, yet another mode coupling occurs due to this flaw. Hence, wave propagation in damaged stiffened composite structure is quite complex. Further, the FE based models are computationally expensive, when used for the wave propagation analysis. In a conventional FE analysis, the maximum possible size of the finite element depends on the wavelength of the propagating wave [6-7]. Hence, for high frequency wave propagation analysis, a very dense finite element mesh is inevitable to accurately simulate the wave propagation including the effects of wave scattering at structural discontinuities. Note that SFEM eliminates this problem completely and does not place any restriction on the frequency. More details of SFEM is found in [7] In the present work, we model the built up stiffened structure as the assembly plate spectral elements, wherein we use the plate spectral element reported in [8] as the basic building block.

Damage detection in built up composite structure is a yet another challenging task due to the complex nature of wave scattering. In this work, we propose a method, which uses the developed built up spectral element model and measured responses to locate the damages. This method we call it as Damage Force Indicator (DFI)

The paper is organized as follows. In the next section, description of the development of plate element, using SFEM is given, which is followed by the brief description of the method of modeling built-up structures. The SFEM model thus developed for built-up structures is then used to perform the high frequency wave propagation analysis of a healthy skin-stiffener structure. The responses obtained using the SFEM model is first validated with 2D FE results and the model is then used to detect the damage due to debonding in a skin-stiffener structure using the method of DFI.

SPECTRAL ELEMENT FORMULATION OF COMPOSITE PLATES

Spectral composite plate formulation is reported in [7] and [8]. Here, the formulation is briefly discussed for completeness. The governing equations for a plate for FLPT can be obtained by applying Hamilton's principle and they can be written as

$$\frac{\partial N_{xx}}{\partial x}+\frac{\partial N_{xy}}{\partial y}=I_0\frac{\partial^2 u}{\partial t^2}-I_1\frac{\partial^2 \phi}{\partial t^2},\quad \frac{\partial N_{xy}}{\partial x}+\frac{\partial N_{yy}}{\partial y}=I_0\frac{\partial^2 v}{\partial t^2}-I_1\frac{\partial^2 \psi}{\partial t^2},\quad \frac{\partial V_x}{\partial x}+\frac{\partial V_y}{\partial y}=I_0\frac{\partial^2 w}{\partial t^2}$$

$$\frac{\partial M_{xx}}{\partial x}+\frac{\partial M_{xy}}{\partial y}=I_2\frac{\partial^2 \phi}{\partial t^2}-I_1\frac{\partial^2 u}{\partial t^2},\qquad \frac{\partial M_{xy}}{\partial x}+\frac{\partial M_{yy}}{\partial y}=I_2\frac{\partial^2 \psi}{\partial t^2}-I_1\frac{\partial^2 v}{\partial t^2} \tag{1}$$

where the mass moments are defined by

$$[I_0,I_1,I_2]=\int_A \rho[1,Z,Z^2]dA \tag{2}$$

The associated stress resultants for this problem is given by

$$\begin{aligned}&\bar{N}_{xx}=N_{xx}n_x+N_{xy}n_y,\quad \bar{N}_{yy}=N_{xy}n_x+N_{yy}n_y,\quad \bar{V}_x=V_xn_x+V_yn_y\\&\bar{M}_{xx}=-M_{xx}n_x-M_{xy}n_y,\quad \bar{M}_{yy}=-M_{xy}n_x-M_{yy}n_y\end{aligned} \tag{3}$$

where, $\bar{N}_{xx}$ and $\bar{N}_{yy}$ are normal force resultants in the two coordinate directions, while the $\bar{M}_{xx}$ and $\bar{M}_{yy}$ are the corresponding moment resultants and $\bar{V}_x$ is the shear force resultant in the thickness direction. These are shown in Fig.1

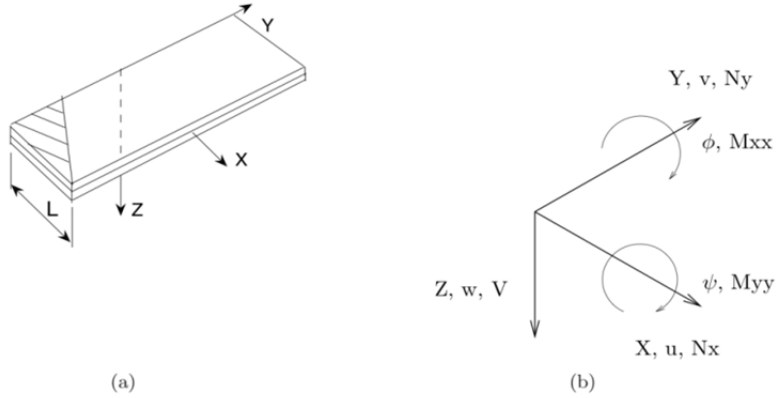

Figure 1 (a) Plate geometry (b) Degrees of freedom for a general plate spectral element.

The spectral element formulation begins by assuming harmonic waves in the time and space (Fourier series is employed in Y direction in which the model is unbounded), i.e.

$$\begin{Bmatrix} u(x,y,t) \\ v(x,y,t) \\ w(x,y,t) \\ \phi(x,y,t) \\ \psi(x,y,t) \end{Bmatrix} = \left[\sum_{n=1}^{N} \sum_{m=1}^{M} \begin{Bmatrix} \hat{u}(x,\omega_n) \\ \hat{v}(x,\omega_n) \\ \hat{w}(x,\omega_n) \\ \hat{\phi}(x,\omega_n) \\ \hat{\psi}(x,\omega_n) \end{Bmatrix} \begin{Bmatrix} \cos(\eta_m y) \\ \sin(\eta_m y) \end{Bmatrix} \right] e^{-j\omega_n t} \quad (4)$$

where *u, v*, and *w* are the displacement components of the reference plane, in the *X, Y*, and *Z* direction, respectively, and $\hat{u}$, $\hat{v}$ and $\hat{w}$ are its transform in Fourier domain. Similarly φ and ψ are the rotations of the reference plane about *Y* and *X-axis*, respectively and $\hat{\phi}$, $\hat{\psi}$ are its transform in Fourier domain. Here, $\boldsymbol{\omega_n}$ is the discrete angular frequency and $\boldsymbol{\eta_m}$ is the discrete horizontal wavenumber ($\boldsymbol{\eta_m = 2\pi(m-1)/Y}$, Y is the length in Y direction). Substituting Equation (4) in Equation (1), a polynomial eigenvalue problem is obtained to find the wave number *k* and the wave amplitude as

$$\psi(k)v = (k^2 A_2 + kA_1 + A_0)v = 0 \quad (5)$$

where *k i*s the eigenvalue and *v* is the corresponding right eigenvector and A_i is 5× 5 matrix, which can be written in terms of the material properties. Wavenumber and the wave amplitudes are computed by a method based on companion matrix and the singular value decomposition (SVD). The force vector is evaluated at the nodes (substituting nx = ±1), to obtain the nodal force vectors. Final equation, which shows the relation between the nodal force and nodal displacement vector at frequency $\boldsymbol{\omega_n}$ and wavenumber $\boldsymbol{\eta_m}$ can be written as,

$$\{\hat{f}\}_{n,m} = [\hat{K}]_{n,m} \{\hat{u}\}_{n,m} \quad (6)$$

where $[\hat{K}]_{n,m}$ is the dynamic stiffness matrix at frequency $\boldsymbol{\omega_n}$ and wavenumber $\boldsymbol{\eta_m}$ of order 10 × 10, $\{\hat{u}\}_{n,m}$ and $\{\hat{f}\}_{n,m}$ are nodal force and displacement vectors, respectively. Further details of the modeling have been explained in detail in [8].

MODELING OF STIFFENED STRUCTURES

The formulated spectral plate element can also be employed for modeling built-up structures such as skin-stiffener type structures (Fig. 2 (a)), which are essential as far as aircraft structures are concerned. The stiffened structure can be modeled as an assemblage of number of plate elements. However, for analyzing three-dimensional structures, it is necessary to transform the stiffness matrix from the local element coordinate to the global coordinate. The method of assembling a plate with stiffener is shown in Fig 2(b). Here, skin is modeled with a plate element (1-2, Fig. 2(b)) and its stiffness matrix can be obtained in the global coordinates

(local coordinates coincides with global coordinates, *XYZ* as in Fig. 2(b)). Stiffener is at an angle 90^0 (anticlockwise) to the skin element 1-2 and is modeled using a plate element 2-3. The transformed coordinate system ($X_1Y_1Z_1$, Fig 2(b)) for the stiffener element formulation is obtained by rotating the global coordinate system (*XYZ*), by 90^0 anticlockwise. Hence, before assembling the elements 1-2 and 2-3, the stiffness matrix of the element 2-3, which is obtained in the local coordinate system ($X_1Y_1Z_1$) is transformed in to global (*XYZ*) coordinate system using a transformation matrix *T* of order 10 × 10 given by

$$[T]=\begin{bmatrix} [Q] & [0] \\ [0] & [Q] \end{bmatrix},\quad [Q]=\begin{bmatrix} \cos\theta & 0 & \sin\theta & 0 & 0 \\ 0 & 1 & 0 & 0 & 0 \\ -\sin\theta & 0 & \cos\theta & 0 & 0 \\ 0 & 0 & 0 & 1 & 0 \\ 0 & 0 & 0 & 0 & 1 \end{bmatrix}, \qquad (7)$$

$$[K_g]_{n,m}=[T]^T[K_l]_{n,m}[T]$$

where $[K_l]_{n,m}$ is the element stiffness matrix in the local coordinate system ($X_1Y_1Z_1$) and $[K_g]_{n,m}$ is the transformed stiffness matrix in global coordinates (*XYZ*) at each *n* and *m* (ω_n and η_m) and θ is the rotation of the plate with respect to Y axis. The stiffened structure shown in Fig 2, is modeled by assembling spectral plate elements, 1-2, 2-3, and 2-4 and the global stiffness matrix is of the order 20 × 20.

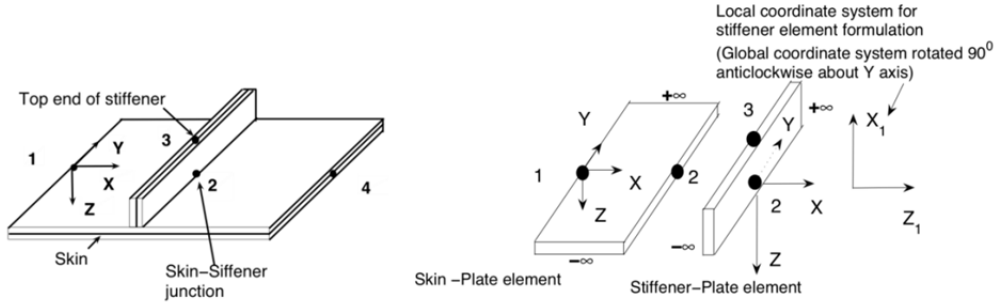

(a) **(b)**

Figure 2 (a) Stiffened aircraft structure (b) Plate element assembly

RESULTS AND DISCUSSION

In this section, we will perform our analysis on a structure shown in Fig 2(a). The material property of the structure is as follows: E_1 =144.48 Gpa, $E_2 = E_3$ =9.63 Gpa, $G_{23} = G_{13} = G_{12}$ =4.128 GPa, ν_{23} =0.3, $\nu_{13} = \nu_{12}$ = 0.02 and ρ=1389 kg/m^3, which are the properties corresponding to GFRP. Each plate is assumed to be made of 8 layers with each ply being 1 mm.

The SFEM model developed is first validated by comparing the transverse velocity responses of a stiffened structure obtained using the model with that of the responses obtained from 2D FE model. In SFEM, to model a skin stiffener structure with one stiffener (Fig. 2(a)), three spectral plate elements are required, which results in a system matrix of order 20. Skin stiffener structure used for the study is 0.8 m in *X*-direction, 1.2 m in Y direction and a stiffener of 0.5 m height is attached

at 0.6 m away (in *X*-direction) from node 1 (Fig. 2(a)). In SFEM, load is transformed in frequency domain by the FFT, where 8192 (N in Equation (4)) sampling points are used. For spatial variation, 30 Fourier series coefficients (M in Equation (4)) are considered. In FE analysis, structure is modeled using 4- noded plate elements and to model the symmetric part of the skin-stiffener structure, having geometric parameters as mentioned above, the analysis requires approximately 10000 elements. While solving via FE analysis, Newmark's time integration method is adopted with a time increment of 1 μs.

Wavenumber computed from Equation (5) gives both symmetric (S_0 mode) and anti-symmetric (A_0 mode) guided wave modes, which can travel over long distances interacting with damages if any giving rises to mode coupling. To obtain these modes, we apply a broadband load in the transverse direction at node 1 (Fig 2(a)) with node 4 being fixed. The transverse velocity response at node 1 (Fig. 2 (a)) of the skin-stiffener structure obtained, using both SFEM and regular FE method, is shown in Fig. 3, where refection (A_0 mode) from the junction of skin and stiffener (node 2, Fig. 2(a)) starts at 0.62 ms and the refection (S_0 mode) from the top free end of stiffener (node 3, Fig. 2), which is present due to the flexural-axial coupling, starts at 0.72 ms (marked in circle, Figure 3(a)). In wave propagation analysis, the time gap between the incident pulse and the time for first refection is a measure of the group speeds. Hence, if we know the distance traveled by the wave and the time gap between the incident pulse and reflected pulse, we can obtain the speed of the wave. Here, in the present study, the symmetric axial mode travels (at 10000 m/s) five times faster than the antisymmetric flexural mode. In the plot, an excellent match can be observed between the SFEM and regular FE response, which establishes the accuracy of the SFEM model, developed for the stiffened structures.

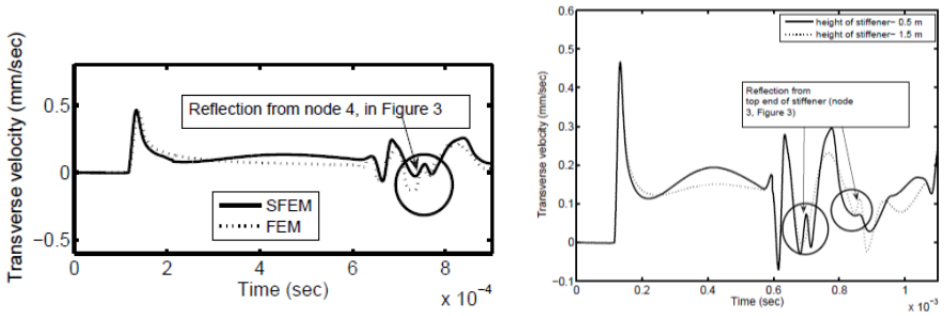

(a) (b)

Figure 3 (a) Comparison of SFEM and FEM Models (b) SFEM responses for different stiffener heights

Next, we will see the wave scattering for different stiffener heights, which is shown in Figure 3(b). Even though the applied load is in the transverse direction, due to the flexural-axial coupling, S_0 mode is generated in the stiffener and the trace of this mode can also be seen in the transverse velocity response of the skin-stiffener structure. The reflections (marked in circles, in Fig. 3(b)) from the stiffener top (node 3, in Fig. 2(a)) starts at 0.7 ms, in a 0.5 m high stiffener, where as in a 1.5 m high stiffener, the reflection will only start at 0.85 ms.

DEBOND DETECTION IN STIFFENED STRUCTURE USING DFI

The concept of damage force indicator [6], which is being derived from the dynamic stiffness matrix of the healthy structure along with the nodal displacements of the debonded stiffened structure, can be used for identifying the region of debond. Here, the damage can be located within the region of application of the sensing points. In SFEM, a healthy plate of any length, in a structure can be modeled using a single spectral plate element. Hence, for the damage force calculation, compared to the conventional FEM, the SFEM model requires only very less number of sensor points. Here, the dynamic stiffness matrix of the healthy stiffened structure obtained from the SFEM model and the nodal displacements obtained experimentally, are used to compute the damage force indicators. The damage force indicator can be defined as,

$$\{\Delta\hat{f}\} = [\hat{K}]_h \{\hat{u}\}_d - \{\hat{f}\}_d \qquad \textbf{(8)}$$

where the subscript *h* stands for the healthy structure (stiffened structure with no debond) and the subscript *d* stands for the structure with debond. $[\hat{K}_h(\omega_n)]$ is the global dynamic stiffness matrix at each FFT sampling frequency ω_n, which can be obtained using the SFEM model discussed in section 3 and the velocity response from the debonded structure, $\{\hat{u}_d\}$ is obtained experimentally, which is adequately filtered to remove the unwanted white noise. The values of vector $\{\Delta\hat{f}\}$ associated with the degrees of freedom (dofs) of the damaged elements (element 2-3, Fig. 2(a)) will be non-zero. The damage force indicator vector *d* of length *m* (m is the total number of dofs in the model) can be written as

$$\{d_i\} = \sum_{\omega_n} |R_{ii}|, \quad i \in [1, m] \quad n = 1, \ldots, N \qquad \textbf{(9)}$$

where

$$[\hat{R}(\omega_n)] = \{\Delta\hat{f}\}^T \{\Delta\hat{f}\}^* \qquad \textbf{(10)}$$

$[\hat{R}(\omega_n)]$ is an *m* x *m* square matrix and $\{\Delta\hat{f}\}^*$ is the transpose of the complex conjugate of the $\{\Delta\hat{f}\}$. In this method, if the i_{th} element includes the damaged area, there will be non-zero diagonal entries in the $[\hat{R}(\omega_n)]$, corresponding to the dofs associated with the i_{th} element and the rest of the entries will be zero. Magnitude of these non-zero diagonal entries will depend on the applied load, and the configuration of the debonded region. Damage force indicator vector *d* is thus the sum of absolute values of the diagonal entries in $[\hat{R}(\omega_n)]$ over all frequency steps ***n*=1, ..., *N* (*N*=**nyquist frequency in FFT**).**

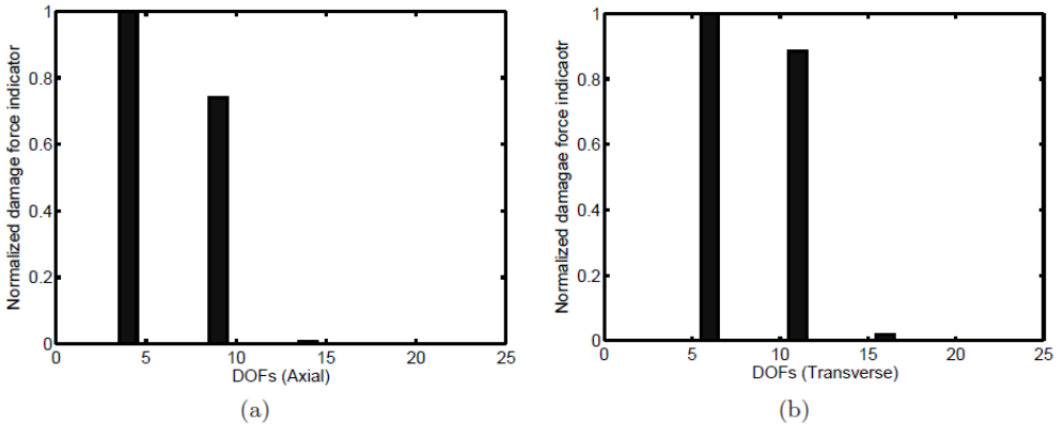

Figure 4 Normalized DFI (a) corresponding to axial dof (b) corresponding to transverse dof.

The nodal displacements obtained experimentally are first converted to frequency domain before we actually multiply it with the dynamic stiffness matrix of the healthy stiffened structure, obtained using SFEM model. The value of damage force (*d*) is normalized with respect to Max (*d*), separately for axial and transverse dofs. A broad band load is used for the study. The material and geometric properties are same as that we used previously. The plots of the normalized damage force indicator, for a stiffened structure with a debond (length in Y direction= 60 cm and the length in z direction= 2 cm), is shown in Fig. 4, where, the normalized damage force indicators for axial and transverse dofs are shown and we can see that the dofs (dofs-4, 9 and 14 (axial, Fig. 4(a)) and dofs-6,11 and 16 (transverse, Fig. 4(b)) corresponding to the debonded region show peaks, which indicate the presence of debond in the structure. However, the peaks of dofs corresponding to node 4 (Fig. 2(a)) in the skin (dof 14 (axial, Fig. 9(a)) and dof 16 (transverse, Fig. 4(b))), are very small compared to the peaks of the dofs corresponding to the stiffener (dofs 4 and 9 (axial, Fig. 4(a)) and dofs 6 and 11 (transverse, Fig 4(b)). The result shows that the method of damage force indicator is effective in locating the region of debond in a composite stiffened structure.

CONCLUSIONS

A model is developed to study the wave propagation in stiffened structures, using the concept of assembling the 2D plate elements, which are spectrally formulated. The method of assembling the plate elements to model a stiffened structure is very simple and straight forward. The SFEM model shows excellent match with the 2D FE results. Further, the model requires only small system size and consequently less computational time, compared to 2D FE analysis while solving high frequency wave propagation problems of stiffened composite structures. The effect of flexural-axial coupling on the wave responses are well captured using the SFEM model. The model is capable of modeling a skin with multiple stiffeners. The method of damage force indicator applied to the present SFEM model is found to be effective in locating the region of debond, in a stiffened structure.

ACKNOWLEDGEMENT

The author would like to thank his graduate student Mr V Ajith and the Boeing Aircraft Company, (St Louis, USA), for supporting this work.

REFERENCES

1. Rathod, V.T. and Mahapatra, D.R., "Lamb wave based monitoring of plate stiffener debonding using using a circular array of piezo electric sensors", Int. J. on Smart Sensing and Intelligent Systems, 3(1), 27-44 (2010)
2. Grondal, S., Assaad, J., delebarre, C., Moulin, E., "Health monitoring of a composite wing box structure",Ultrasonics, 42, 819-824 (2004).
3. Edward, A.S. and Samer, A.T., "A finite element model for the analysis of stiffened laminated plates", Comput. Struct., 75(4) 369-383 (2000).
4. Gangadhara, P.B, "Linear static analysis of hat-stiffened laminated shells using finite elements", Finite elem. anal. des., 39, 1125-1138 (2003).
5. Tran Ich Thinh and Ngo Nhu Khoa, "Free vibration analysis of stiffened laminated plates using a new stiffened element", Technische Mechanik, 28(3-4), 227-236 (2008).
6. S. Gopalakrishnan, A. Chakraborty, D.R. Mahapatra, Spectral Finite Element Method, Springer-Verlag, New York, (2008).
7. Horr, A.M. and Safi, M., "Full dynamic analysis of offshore platform structures using exact Timoshenko pipe element", Transactions of the ASME, 125(3), 168-175 (2003).
8. Chakraborty, A. and Gopalakrishnan, S., "A Spectral finite element model for wave propagation analysis in laminated composite plate", J. Vib. Acoust., 128, 477-488 (2006)